J. Fluid Mech. (2005), *vol.* 541, *pp.* 371–381.
doi:10.1017/S0022112005005963 Printed in the United Kingdom

Fluid kinematics on a deformable surface

By J.-Z. WU[1,2]†, Y.-T. YANG[1], Y.-B. LUO[1] AND C. POZRIKIDIS[3]

[1]State Key Laboratory for Turbulence and Complex System, Peking University, Beijing 100871, China

[2]University of Tennessee Space Institute, Tullahoma, TN 37388, USA

[3]University of California, San Diego, La Jolla, CA 92093-0411, USA

(Received 4 February 2005 and in revised form 17 February 2005)

An expression for the rate-of-strain tensor on a rigid surface due to Caswell is generalized to an arbitrarily moving and continuously deforming surface or interface between two immiscible fluids. Corresponding expressions for the velocity gradient and vorticity tensors are derived in an inertial frame of reference. A noteworthy feature of the expression for the rate-of-strain tensor is the presence of a tangent-tangent component, which is absent in the case of a rigid surface. Kinematic applications based on numerical solutions of the Navier–Stokes equation for laminar and turbulent flow demonstrate the significance and implications of the derived expressions.

1. Introduction

The study of fluid dynamics in the presence of a deformable surface is motivated by applications in rheology, multi-phase and particulate flow, biofluiddynamics, and flow control by the motion of flexible walls. One aspect of the problem is concerned with the kinematics of the deformable surface itself, whether this be a regular interface, an interface populated by a surfactant, an elastic sheet, or a viscoelastic membrane (e.g. Scriven 1960; Aris 1962; Evans & Skalak 1980; Secomb & Skalak 1982; Waxman 1984; Barthès-Biesel & Sgaier 1985; Slattery 1990; Edwards, Brenner & Wasan 1991). Another aspect is concerned with the derivation of dynamical interfacial conditions involving the normal and tangential components of the surface stress on a rigid or deforming surface, and the jump thereof across a fluid interface (e.g. Batchelor 1967; Pozrikidis 1997). Surprisingly, even though such conditions have been derived for specific types of surfaces on several occasions, a general formulation of the kinematic condition applicable under all circumstances is not available.

Consider flow past a rigid surface where the no-slip and no-penetration conditions apply. Caswell (1967) showed that, in the frame of reference fixed on the surface, such that the velocity $\boldsymbol{u}$ is zero over the surface, the boundary value of the rate-of-deformation tensor, $\boldsymbol{D} \equiv \frac{1}{2}(\nabla \boldsymbol{u} + \nabla \boldsymbol{u}^T)$, is given by

$$\boldsymbol{D} = \vartheta \boldsymbol{n}\boldsymbol{n} + \tfrac{1}{2}[\boldsymbol{n}(\boldsymbol{\omega} \times \boldsymbol{n}) + (\boldsymbol{\omega} \times \boldsymbol{n})\boldsymbol{n}], \tag{1.1}$$

where $\vartheta = \nabla \cdot \boldsymbol{u}$ is the rate of dilatation, $\boldsymbol{\omega} = \nabla \times \boldsymbol{u}$ is the vorticity, and $\boldsymbol{n}$ is the unit normal vector. The last two terms on the right-hand side of (1.1) enclosed by the square brackets express the traceless deviatoric part of the rate-of-strain tensor, $\boldsymbol{n} \cdot (\boldsymbol{\omega} \times \boldsymbol{n}) = 0$. Viewed in a frame of reference in which the rigid surface rotates with angular velocity $\boldsymbol{w}(t)$, expression (1.1) takes an identical form, except that the vorticity

† Author to whom correspondence should be addressed: jzwu@mech.pku.edu.cn, jzwu@utsi.edu

is replaced by the relative vorticity, $\boldsymbol{\omega}_r \equiv \boldsymbol{\omega} - 2\boldsymbol{w}$. Because of the no-slip boundary condition, $\boldsymbol{\omega}_r$ is a purely tangent vector. Caswell's formula implies an expression for the shear stress in a Newtonian fluid, $\boldsymbol{\tau} = \mu\boldsymbol{\omega}_r \times \boldsymbol{n}$, where μ is the fluid viscosity, which is tantamount to the more familiar expression $\boldsymbol{\tau} = \mu\boldsymbol{n}\cdot(\nabla\boldsymbol{u})\cdot\boldsymbol{P}$, where $\boldsymbol{P} \equiv \boldsymbol{I} - \boldsymbol{nn}$ is the tangential projection matrix.

The main goal of this paper is to generalize expression (1.1) to a deformable surface. The kinematics of the deformable surface itself under the influence of a specified velocity field is a prerequisite for the new developments. Most previous authors worked with kinematic expressions in surface (intrinsic) curvilinear coordinates. The invariant formulation was reviewed by Wu & Wu (1996, referred to WW96 hereafter), as summarized in § 2 of this paper. New formulas for the velocity gradient tensor and its symmetric and skew-symmetric components on a deformable surface are derived in § 3, kinematic applications are presented in § 4, and the new contributions are summarized in § 5.

2. Kinematics of a deformable surface

Consider a small material surface patch with surface area, δS, and introduce the differential material normal vector $\delta\boldsymbol{S} = \boldsymbol{n}\delta S$. The rate of change of $\delta\boldsymbol{S}$ is given by the material derivative

$$\frac{1}{\delta S}\frac{\mathrm{D}\delta\boldsymbol{S}}{\mathrm{D}t} = \boldsymbol{n}\,\frac{1}{\delta S}\frac{\mathrm{D}\delta S}{\mathrm{D}t} + \frac{\mathrm{D}\boldsymbol{n}}{\mathrm{D}t} = \boldsymbol{n}\,r_s + \boldsymbol{w}\times\boldsymbol{n}, \tag{2.1}$$

where r_s is the rate of change of δS, and $\boldsymbol{w}(x,t)$ is the angular velocity of the convected unit normal vector, $\boldsymbol{n}$. In terms of the surface rate-of-deformation tensor defined as

$$\boldsymbol{B} \equiv \vartheta\,\boldsymbol{I} - (\nabla\boldsymbol{u})^T \tag{2.2}$$

(e.g. Dishington 1965), the rate of change of the material normal vector is given by

$$\frac{1}{\delta S}\frac{\mathrm{D}\delta\boldsymbol{S}}{\mathrm{D}t} = \boldsymbol{n}\cdot\boldsymbol{B} = -(\boldsymbol{n}\times\nabla)\times\boldsymbol{u}. \tag{2.3}$$

The expression on the right-hand side was derived by T. Y. Wu, as stated in a footnote to WW96. Because the operator $\boldsymbol{n}\times\nabla$ involves tangential derivatives alone, only the surface distribution of the velocity is required to evaluate the rate of change of the material normal vector, in agreement with physical intuition. Consequently, the rate of change of the material normal vector can be expressed solely in terms of the known instantaneous geometry and motion of the surface, and is independent of the flow off the surface. After some manipulation, the evolution law (2.3) yields the expression

$$r_s = \nabla_\pi\cdot\boldsymbol{u} = \nabla_\pi\cdot\boldsymbol{u}_\pi - Ku_n, \tag{2.4}$$

together with expressions for the tangential and normal components of $\boldsymbol{w}$,

$$\boldsymbol{w}_\pi = -\boldsymbol{n}\times(\nabla_\pi u_n + \boldsymbol{u}\cdot\boldsymbol{K}), \qquad \boldsymbol{w}_n = \frac{1}{2}[(\boldsymbol{n}\times\nabla)\cdot\boldsymbol{u}]\boldsymbol{n}, \tag{2.5}$$

where $\nabla_\pi \equiv \boldsymbol{P}\cdot\nabla$ is the surface gradient, $\boldsymbol{u}_n \equiv (\boldsymbol{u}\cdot\boldsymbol{n})\boldsymbol{n} = u_n\boldsymbol{n}$ is the normal velocity, $\boldsymbol{u}_\pi \equiv \boldsymbol{P}\cdot\boldsymbol{u} = \boldsymbol{n}\times(\boldsymbol{u}\times\boldsymbol{n})$ is the tangential velocity, $\boldsymbol{K} = -\nabla_\pi\boldsymbol{n}$ is the curvature tensor, and $K = -\nabla_\pi\cdot\boldsymbol{n} = \mathrm{Tr}(\boldsymbol{K})$ is twice the mean curvature. The decompositions (WW96)

$$\nabla\boldsymbol{u} = \vartheta\boldsymbol{I} + 2\boldsymbol{\Omega} - \boldsymbol{B}, \qquad \boldsymbol{D} = \vartheta\boldsymbol{I} + \boldsymbol{\Omega} - \boldsymbol{B}, \tag{2.6}$$

will considerably simplify the impending derivation of formulae for the rate-of-strain and velocity gradient tensors; $\boldsymbol{\Omega}$ is the vorticity tensor. A key observation is that $\boldsymbol{n}\cdot\boldsymbol{B}$ evaluated at the surface is expressible in terms of the velocity over, and geometry of, the surface.

3. Theory

We begin by recasting the expression for the velocity gradient tensor given in (2.6) in the form

$$\nabla \boldsymbol{u} = \boldsymbol{n}(\boldsymbol{n}\cdot\nabla\boldsymbol{u}) + \boldsymbol{P}\cdot\nabla\boldsymbol{u} = \boldsymbol{n}\boldsymbol{n}\vartheta + \boldsymbol{n}(\boldsymbol{\omega}\times\boldsymbol{n} - \boldsymbol{n}\cdot\boldsymbol{B}) + \nabla_\pi \boldsymbol{u}, \tag{3.1}$$

where $\vartheta = r_s + u_{n,n}$, and $u_{n,n} = \boldsymbol{n}\cdot(\nabla\boldsymbol{u})\cdot\boldsymbol{n}$ is the normal derivative of the normal velocity component. For flow over a stationary rigid surface, the last two terms of (3.1) are zero, yielding

$$\nabla \boldsymbol{u} = \boldsymbol{n}\boldsymbol{n}\vartheta + \boldsymbol{n}(\boldsymbol{\omega}\times\boldsymbol{n}), \tag{3.2}$$

from which Caswell's formula (1.1) immediately follows. Moreover, because $r_s = 0$, ϑ can be replaced by the normal derivative $u_{n,n}$.

The kinematics associated with surface deformability is encapsulated in the last two terms on the right-hand side of (3.1). Since $\boldsymbol{n}\cdot\boldsymbol{B}$ in the penultimate term is given in (2.1) and (2.3), we carry out the normal-tangential (N-T) decomposition of $\nabla_\pi \boldsymbol{u}$ by way of projection from the right. Using (2.5), we obtain the tangential-tangential (T-T) tensor

$$(\nabla_\pi \boldsymbol{u})\cdot\boldsymbol{P} \equiv (\nabla_\pi \boldsymbol{u})_\pi, \tag{3.3}$$

and the T-N tensor

$$(\nabla_\pi \boldsymbol{u}\cdot\boldsymbol{n})\boldsymbol{n} = (\nabla_\pi u_n - \boldsymbol{u}\cdot\nabla_\pi \boldsymbol{n})\boldsymbol{n} = -(\boldsymbol{w}\times\boldsymbol{n})\boldsymbol{n}. \tag{3.4}$$

Substituting these expressions in (3.1), and using (2.2) and (2.5) to evaluate $\boldsymbol{n}\cdot\boldsymbol{B}$, we find

$$\nabla \boldsymbol{u} = \boldsymbol{n}\boldsymbol{n}u_{n,n} + \boldsymbol{n}(\boldsymbol{\omega}\times\boldsymbol{n}) - [\boldsymbol{n}(\boldsymbol{w}\times\boldsymbol{n}) + (\boldsymbol{w}\times\boldsymbol{n})\boldsymbol{n}] + (\nabla_\pi \boldsymbol{u})_\pi, \tag{3.5}$$

which generalizes (3.2). Note that r_s in the normal-normal (N-N) component expressed by the first term on the right-hand side has been cancelled.

Let $\boldsymbol{S}$ and $\boldsymbol{A}$ be the symmetric and skew-symmetric parts of $(\nabla_\pi \boldsymbol{u})_\pi$. By (3.5), we derive

$$\boldsymbol{D} = \boldsymbol{n}\boldsymbol{n}u_{n,n} + \tfrac{1}{2}\boldsymbol{n}(\boldsymbol{\omega}_r\times\boldsymbol{n}) + \tfrac{1}{2}(\boldsymbol{\omega}_r\times\boldsymbol{n})\boldsymbol{n} + \boldsymbol{S}, \tag{3.6}$$

which generalizes (1.1), and a companion expression for the vorticity tensor,

$$\boldsymbol{\Omega} = \tfrac{1}{2}\boldsymbol{n}(\boldsymbol{\omega}\times\boldsymbol{n}) + \tfrac{1}{2}(\boldsymbol{\omega}\times\boldsymbol{n})\boldsymbol{n} + \boldsymbol{A}. \tag{3.7}$$

Equations (3.5)–(3.7) represent the main new theoretical result, which is the intrinsic decomposition of $\nabla\boldsymbol{u}$, $\boldsymbol{D}$, and $\boldsymbol{\Omega}$ into normal and tangential components that afford a physical representation. Specifically, the N-N component is associated with the normal derivative of the normal velocity component, the N-T and T-N components are associated with the relative vorticity, and the T-T component is associated with surface flexibility. The last component is independent of the global structure of the flow. Given the boundary distribution of the velocity, these formulae allow us to describe the motion and deformation of a fluid element near the surface by considering only three independent components of the velocity gradient tensor, i.e. $u_{n,n}$ and the two independent components of the solenoidal vorticity vector. In the Appendix, the components of the new tensors $(\nabla_\pi \boldsymbol{u})_\pi$, $\boldsymbol{S}$, and $\boldsymbol{A}$, are presented in surface orthonormal coordinates, and it is demonstrated that $\boldsymbol{A}$ is precisely the T-T vorticity tensor, whereas the surface curvature tensor $\boldsymbol{K}$ appears in $\boldsymbol{S}$ only if the normal velocity component is non-zero.

Equation (3.6) suggests that it is most convenient to describe the components of $\boldsymbol{D}$ in intrinsic orthonormal surface coordinates consisting of the normal vector $\boldsymbol{n}$, the

tangent vector $\boldsymbol{\omega}_r$, and their Cartesian complement. Let $\hat{\boldsymbol{n}} = -\boldsymbol{n}$ point into the fluid, and introduce two tangent unit vectors $\boldsymbol{e}_2 = \boldsymbol{\omega}_r/\omega_r$ and $\boldsymbol{e}_1 = \boldsymbol{e}_2 \times \hat{\boldsymbol{n}}$, the latter pointing along the skin friction field, $\boldsymbol{\tau}_w = \mu\boldsymbol{\omega}_r \times \hat{\boldsymbol{n}}$, for a Newtonian fluid. This frame is called the $\boldsymbol{\tau}$-frame by Wu *et al.* (2000). In terms of the triad $(\boldsymbol{e}_1, \boldsymbol{e}_2, \boldsymbol{n})$, expression (3.6) is

$$\boldsymbol{D} = \begin{bmatrix} S_{11} & S_{12} & \omega_r/2 \\ S_{12} & r_s - S_{11} & 0 \\ \omega_r/2 & 0 & u_{n,n} \end{bmatrix}. \tag{3.8}$$

For example, consider a two-dimensional incompressible uniform flow past an infinite flexible wall executing transverse oscillations with angular frequency, n, due to a travelling wave. In a laboratory-fixed frame $(\hat{x}, \hat{y})$, the wall profile is given by

$$\hat{y}_w = f(k\hat{x} - nt) = f[k(\hat{x} - ct)], \tag{3.9}$$

where $f(x)$ is a periodic function, k is the wavenumber, and $c = n/k$ is the phase velocity. In a frame of reference moving with the wave through the Galilean transformation $x = \hat{x} - ct$ and $y = \hat{y}$, the wall has a stationary profile described by $y_w = f(kx)$, and the Cartesian components of the wall velocity are given by

$$u_w = -c, \qquad v_w = \frac{\mathrm{d}y_w}{\mathrm{d}t} = -ck\,f', \tag{3.10}$$

so that $v_w/u_w = kf' = \mathrm{d}y_w/\mathrm{d}x$, where a prime denotes a derivative with respect to kx. WW96 showed that, at a critical phase velocity, c, the flow can become *naturally periodic*, whereupon it appears steady when viewed in the wave frame. It then follows that $S_{11} = r_s = -u_{n,n}$ and $S_{12} = S_{21} = 0$, so that (3.8) simplifies to

$$D_{ij} = \begin{bmatrix} r_s & 0 & \omega_r/2 \\ 0 & 0 & 0 \\ \omega_r/2 & 0 & -r_s \end{bmatrix}, \tag{3.11}$$

where

$$r_s = \frac{ck^3 f' f''}{1 + k^2 f'^2}, \qquad \omega_r = \omega - 2w = \omega - \frac{2ck^2 f''}{1 + k^2 f'^2}. \tag{3.12}$$

The jump in the hydrodynamic traction across the interface is of particular interest in deriving interfacial conditions involving the surface tension and possibly other surface rheological properties. Consider the product of two scalar, vectorial, or tensorial functions across an interface, f and g, on either side of an interface. The jump of the product across the interface, denoted by $[\![\cdot]\!]$, is given by

$$[\![fg]\!] = [\![f]\!]\,\overline{g} + \overline{f}\,[\![g]\!], \tag{3.13}$$

where the overbar denotes the mean value on either side. We note that $\nabla_\pi \boldsymbol{u}$, $\boldsymbol{n}\cdot\boldsymbol{B}$, r_s, and $\boldsymbol{w}$, remain continuous as the interface is crossed, identify $[\![\boldsymbol{\omega}]\!]$ with $\boldsymbol{\omega}_r$, and use (3.5) and (3.6) to obtain

$$[\![\nabla \boldsymbol{u}]\!] = \boldsymbol{nn}[\![u_{n,n}]\!] + \boldsymbol{n}(\boldsymbol{\omega}_r \times \boldsymbol{n}), \tag{3.14}$$

$$[\![\boldsymbol{D}]\!] = \boldsymbol{nn}[\![u_{n,n}]\!] + \tfrac{1}{2}\boldsymbol{n}(\boldsymbol{\omega}_r \times \boldsymbol{n}) + \tfrac{1}{2}(\boldsymbol{\omega}_r \times \boldsymbol{n})\boldsymbol{n}, \tag{3.15}$$

$$[\![\boldsymbol{\Omega}]\!] = \tfrac{1}{2}[\boldsymbol{n}(\boldsymbol{\omega}_r \times \boldsymbol{n}) - (\boldsymbol{\omega}_r \times \boldsymbol{n})\boldsymbol{n}]. \tag{3.16}$$

These formulas can be used to derive specific expressions for the interfacial force balance according to an assumed interfacial rheology (e.g. Evans & Skalak 1980; Barthès-Biesel & Sgaier 1985; Pozrikidis 2001).

As a further application, we consider the jump in the Eulerian and convective accelerations, $\partial \boldsymbol{u}/\partial t$ and $\boldsymbol{u}\cdot\nabla\boldsymbol{u}$, on either side of the interface. Although continuity of velocity requires $[\![\boldsymbol{u}]\!]=\boldsymbol{0}$ and thus $[\![\boldsymbol{a}]\!]=\mathrm{D}[\![\boldsymbol{u}]\!]/\mathrm{D}t=\boldsymbol{0}$, the individual parts comprising of the aforementioned accelerations are allowed to be discontinuous. Since $[\![\boldsymbol{u}]\!]=\boldsymbol{0}$, we depart from expression

$$[\![\boldsymbol{u}\cdot\nabla\boldsymbol{u}]\!]=u_n\boldsymbol{n}\cdot[\![\nabla\boldsymbol{u}]\!], \tag{3.17}$$

use (3.14), and require $[\![\boldsymbol{a}]\!]=\boldsymbol{0}$, to find

$$[\![\boldsymbol{u}\cdot\nabla\boldsymbol{u}]\!]=-\frac{\partial[\![\boldsymbol{u}]\!]}{\partial t}=u_n(\boldsymbol{n}[\![u_{n,n}]\!]+\boldsymbol{\omega}_r\times\boldsymbol{n}), \tag{3.18}$$

which generalizes a result due to WW96 for a rotating rigid boundary. When $u_n=0$, in which case the interface is stationary, the jumps in both $\boldsymbol{u}\cdot\nabla\boldsymbol{u}$ and $\boldsymbol{u}_{,t}$ disappear.

4. Eigenvalues and principal axes of the rate-of-strain tensor

Although the T-T tensor $\boldsymbol{S}$ does not enter the constitutive equation for the surface stress of a Newtonian fluid, it does contain useful information on the kinematics of the flow near a surface by determining the eigenvalues and principal axes of $\boldsymbol{D}$ near the surface, as suggested by (3.8). To illustrate this point, we consider incompressible flow past a rigid surface in the $\boldsymbol{\tau}$-frame introduced in § 3. Since $r_s=0$, the angles subtended between the stretching or compressive principal axes – namely the first or third principal axes of strain rate tensor, $\boldsymbol{D}$ – and the skin friction vector ($\boldsymbol{e}_1$-direction), are 45° or 135°, respectively, as can be seen from the following expression (4.2). However, if the wall is flexible, r_s is no longer zero, and the angles deviate from these values, as will be demonstrated by two numerical examples.

In the first example, we consider flow over a travelling wavy wall, as discussed in § 3. The eigenvalues and angles subtended between the tangent vector pointing upstream and the stretching/shrinking principal axes $\boldsymbol{p}_{1,3}$, follow from (3.11) and (3.12) as

$$\lambda_{1,3}=\pm\frac{1}{2}\sqrt{4r_s^2+\omega_r^2},\qquad \lambda_2=0, \tag{4.1}$$

and

$$\tan\theta_{1,3}=\frac{-2r_s\pm\sqrt{4r_s^2+\omega_r^2}}{\omega_r}, \tag{4.2}$$

where the relative vorticity, ω_r, is calculated from the flow field. Specifically, we assume that the wall profile described in (3.9) takes the sinusoidal form

$$\hat{y}_w=0.2L\cos[k(\hat{x}_w-0.414Ut)], \tag{4.3}$$

where L is the wavelength, and U is the far-field uniform velocity along the x-axis as $y\to\infty$. The choice $c=0.414U$ is motivated by the discovery that, for wall amplitude $0.2L$, the flow exhibits a natural periodicity that justifies the x-periodicity condition in the numerical simulations (WW96).

The vorticity–stream function formulation was used to solve the Navier–Stokes equation in a two-dimensional domain on a finite difference grid. An orthogonal transformation due to Caponi *et al.* (1982) was adopted to map the physical space onto a rectangular computational domain, and a fractional-step scheme with second-order accuracy in both space and time was implemented to carry out the time integration. The Neumann boundary condition for the vorticity at the wall is enforced in solving the vorticity transport equation (WW96).

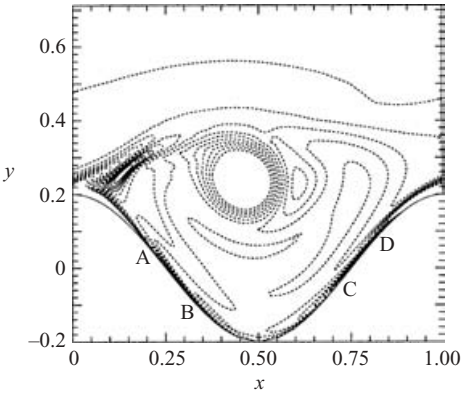

FIGURE 1. Vorticity contours above a sinusoidal wall induced by a boundary wave travelling with phase velocity $c/U = 0.414$. The solid lines are contours of positive vorticity, and the dashed lines are contours of negative vorticity. In figures 1, 2, and 3, the axes have been scaled by the wave length, L.

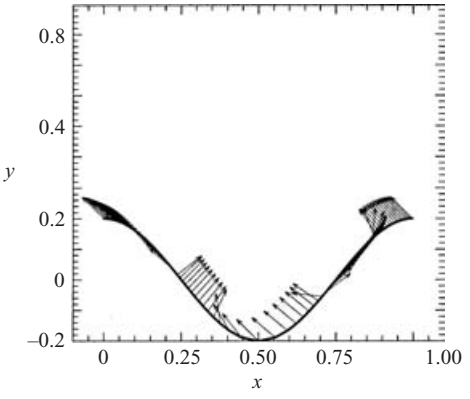

FIGURE 2. Distribution of the stretching principal axis over one period of a sinusoidal wall.

Figure 1 shows the instantaneous vorticity field for Reynolds number $Re \equiv LU/\nu = 5000$, computed on a 128×128 grid. The results show that a boundary layer separates behind the crest of the travelling wave, and the contained vorticity rolls into the wave troughs to form a strong and stable vortical structure. In the wave-fixed frame, the fluid is induced to move upstream below the vortex array in the direction of the wall motion. Because the induced velocity on the wall is not equal to $q_w \equiv \sqrt{u_w^2 + v_w^2}$, a weak periodic near-wall vortex layer remains. The vortical region forms a fluid 'sheath' or 'roller-bearing' separating the near-wall layer from the main stream, which lowers the total drag mainly by reducing the pressure drag.

Figure 2 shows a graph of the principal axis over one period of the wall, $\boldsymbol{p}_1$, and figure 3 shows a corresponding graph of the inclination angle, θ_1. Four regions can be identified within each wavelength, separated by points A, B, C, and D, where ω changes sign, as shown in figure 1. The angle θ_1 is nearly $\pm 45^\circ$ over the majority of the wall. Deviations are observed near the separating points where θ_1 departs considerably from $\pm 45^\circ$, as r_s dominates λ_1 and θ_1. Based on these results, we anticipate that, in a real three-dimensional laminar or turbulent flow, any possible disturbance of the streamwise vortices immediately above a travelling wavy wall will behave differently

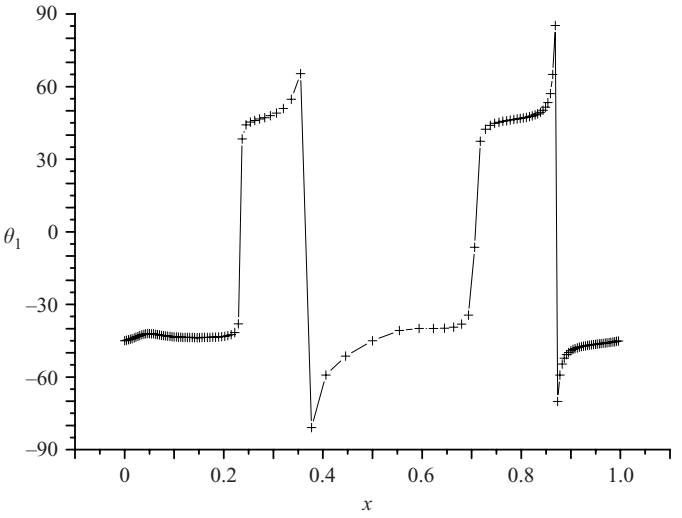

FIGURE 3. Angle subtended between the stretching principal axis and the the tangent vector to the wall (positive in the upstream direction).

from that over a rigid flat or fixed wavy wall. This conjecture will be confirmed in the next example for a simpler flow geometry.

It is well-established that the expected inclination of hairpin vortices in wall-bounded turbulent flow is approximately 45°. Replacing the rigid wall with a flexible surface may significantly affect the morphology of the near-wall coherent structures. Assume that the wall exhibits an in-plane spanwise travelling wavy motion in the $\boldsymbol{e}_z$-direction, i.e. $\boldsymbol{u} = (0, 0, u_z)$, where

$$u_z = f(kz - nt). \tag{4.4}$$

In this case, $\boldsymbol{w} = \boldsymbol{0}$ and

$$S_{\alpha\beta} = \begin{cases} r_s = kf'(kx_2 - nt) & \text{if} \quad \alpha = \beta = 2, \\ 0 & \text{otherwise.} \end{cases} \tag{4.5}$$

Then by (3.8),

$$\lambda_{1,3} = \tfrac{1}{2}\big(-r_s \pm \sqrt{r_s^2 + \omega^2}\big), \quad \lambda_2 = r_s, \tag{4.6}$$

and (4.2) still holds with ω_r replaced by ω.

The effect of the spanwise wavy motion on drag reduction and its significance for the dynamics of flow structures were studied by Zhao, Wu & Luo (2004) by direct numerical simulation of turbulent channel flow. The travelling wave described by (4.4) was found to generate a Stokes-like boundary layer next to the wall, which suppresses the rise of the hairpin heads. Insights into the hairpin-suppression effect can be gained by studying the change of the stretching eigenvalue and principal axis, $\boldsymbol{p}_1$. For this purpose, the numerical method developed by Zhao *et al.* (2004) was applied to conduct further numerical simulations of channel flow. The upper channel wall is stationary, while the lower wall exhibits a spanwise travelling sinusoidal motion described by $u_z = 0.2U\cos(kz - nt)$ with $kh = 1$ and $n^+ = 2\pi/50$, where U is the mean velocity along the x-axis at the channel mid-plane, h is the channel semi-width, and the $^+$ superscript indicates wall units.

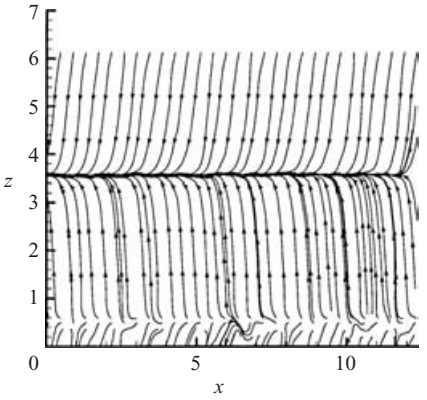

FIGURE 4. Skin-friction lines on a flexible wall exhibiting in-plane oscillations in the spanwise direction in turbulent channel flow. In figures 4, 5, and 6, the axes have been scaled by the channel semi-height.

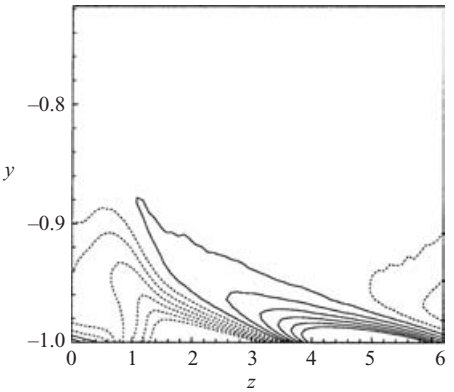

FIGURE 5. Magnification of contours of the streamwise vorticity in the (y,z)-plane near the bottom wall region, averaged in the streamwise direction. The solid contours correspond to positive vorticity, and the dashed contours correspond to negative vorticity.

Figure 4 illustrates the distribution of the instantaneous $\boldsymbol{\tau}_w$-lines on the travelling wall, after Zhao *et al.* (2004, figure 14), exhibiting separation and reattachment lines aligned in the x-direction at positions where $|\omega_x|$ reaches local minima. At the specific time when the data are taken, these are located, respectively, at the dimensionless positions $z_1 \simeq 0.5$ and $z_2 \simeq 3.5$. In the intervening interval, the $\boldsymbol{\tau}_w$-lines are twisted in the $\pm z$-direction. Figure 5 illustrates instantaneous contours of the streamwise average of the vorticity component ω_x near the wall. Note that a change in sign occurs at z_1 and z_2. Figure 6 shows the streamwise average of the angle θ_1 subtended between $\boldsymbol{p}_1$ and $\boldsymbol{e}_1$ (the $\boldsymbol{\tau}_w$-line direction). As in the previous example, a rapid change in θ_1 occurs at z_1 and z_2. Far from the separation and reattachment lines, θ_1 is still close to 45°, as $\omega/2$ dominates the maximum eigenvalue, λ_1. However, since the $\boldsymbol{e}_1$-axis is twisted in the $\pm z$-direction, the formation mechanism of hairpin vortices by streamwise stretching is no longer present. On the other hand, near the separation and reattachment lines, the $\boldsymbol{\tau}_w$-lines are still aligned with the x-axis, even though θ_1 deviates considerably from 45°, as shown in figure 6. Under these circumstances, the stretching of the hairpin vortex is prevented.

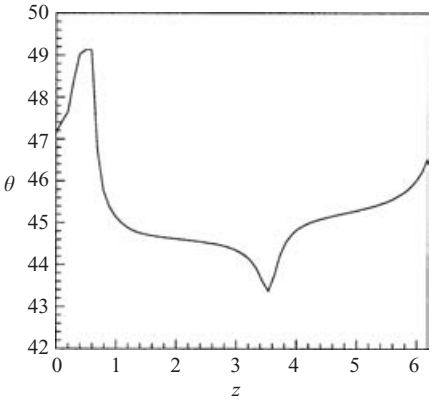

FIGURE 6. Angle subtended between the skin-friction lines and the principal axis of stretching, averaged in the streamwise direction.

5. Conclusions

The kinematics of a fluid on an arbitrarily moving and continuously deforming material surface has been described in terms of the velocity-gradient tensor $\nabla \boldsymbol{u}$, its symmetric part $\boldsymbol{D}$, and skew-symmetric part $\boldsymbol{\Omega}$, evaluated at the surface. General formulae and physical constituents are most easily revealed by using the triple decomposition (2.6) of $\nabla \boldsymbol{u}$. Compared to the kinematics on a rigid surface, the stretching and tilting of a deformable surface make additional contributions to these tensors. In particular, tangent-tangent components of the strain-rate tensor appear. Although these components do not enter directly the expression for the surface stress for a Newtonian fluid, they significantly affect the stretching–shrinking rates and associated principal directions, and thereby influence the near-boundary flow structures and stability of the flow. Overall, the results of this work offer a basis for analysing the interaction of a bulk fluid and a deformable surface in a broad range of applications.

The work is supported in part by National Natural Science Foundation of China under the grant 10172006. C. Pozrikidis was supported by a grant provided by the National Science Foundation.

Appendix. Components of T-T tensors $(\nabla_\pi \boldsymbol{u})_\pi$, $\boldsymbol{S}$, and $\boldsymbol{A}$

Consider an orthogonal curvilinear coordinate system (x_1, x_2, x_3) defined with reference to a surface where axes x_1 and x_2 vary in tangential directions, and the axis x_3 varies in the normal direction. The associated unit vectors are denoted by $\boldsymbol{e}_1$, $\boldsymbol{e}_2$, and $\boldsymbol{e}_3 = \boldsymbol{n}$. The tangential component of the interfacial velocity and curvature tensor can be resolved as

$$\boldsymbol{u}_\pi = u_1 \boldsymbol{e}_1 + u_2 \boldsymbol{e}_2, \qquad \boldsymbol{K} = K_{\alpha\beta} \boldsymbol{e}_\alpha \boldsymbol{e}_\beta, \tag{A 1}$$

where $K_{\alpha\beta} = K_{\beta\alpha}$, for $\alpha, \beta = 1, 2$. To simplify the notation, we denote $\partial_i \equiv (1/h_i)\partial/\partial x_i$ for $i = 1, 2, 3$, where h_i are metric coefficients, under the convention that $h_3 = 1$. The curvatures of the x_1- and x_2-coordinate lines on the wall are given by

$$\left.\begin{aligned} \kappa_1 &\equiv (\partial_1 \boldsymbol{e}_1)\cdot \boldsymbol{e}_2 = -(\partial_1 \boldsymbol{e}_2)\cdot \boldsymbol{e}_1 = -\frac{1}{h_1 h_2}\frac{\partial h_1}{\partial x_2}, \\ \kappa_2 &\equiv (\partial_2 \boldsymbol{e}_2)\cdot \boldsymbol{e}_1 = -(\partial_2 \boldsymbol{e}_1)\cdot \boldsymbol{e}_2 = -\frac{1}{h_1 h_2}\frac{\partial h_2}{\partial x_1}. \end{aligned}\right\} \tag{A 2}$$

If the surface is flat, these are the geometric curvatures of the coordinate lines. Expressions for the derivatives of a vector in this coordinate system are given in equations (14) or (20a) and (20b) of Wu *et al.* (2000).

The tangential velocity-gradient surface tensor can be expressed as

$$(\nabla_\pi \boldsymbol{u})_\pi \equiv (\nabla_\pi \boldsymbol{u})\cdot\boldsymbol{P} = \nabla_\pi(\boldsymbol{u}\cdot\boldsymbol{P}) - \boldsymbol{u}\cdot\nabla_\pi\boldsymbol{P} = \nabla_\pi \boldsymbol{u}_\pi - (\boldsymbol{u}\cdot\boldsymbol{K})n - u_n\boldsymbol{K}. \tag{A 3}$$

The second term in (A3), involving the normal vector, is cancelled by a term hidden in the first term. Using the preceding formulae, the component form of $\nabla_\pi \boldsymbol{u}_\pi$ follows at once as

$$\nabla_\pi \boldsymbol{u}_\pi = \begin{bmatrix} \partial_1 u_1 - \kappa_1 u_2 & \partial_1 u_2 + \kappa_1 u_1 & K_{1\alpha}u_\alpha \\ \partial_1 u_1 + \kappa_2 u_2 & \partial_2 u_2 - \kappa_2 u_1 & K_{2\alpha}u_\alpha \end{bmatrix}. \tag{A 4}$$

Next, we observe that

$$(\boldsymbol{u}\cdot\boldsymbol{K})n = u_\alpha \boldsymbol{K}_{\alpha\beta}\boldsymbol{e}_\beta \boldsymbol{n}, \qquad u_n\boldsymbol{K} = u_n K_{\alpha\beta}\boldsymbol{e}_\alpha\boldsymbol{e}_\beta, \tag{A 5}$$

and find

$$(\nabla_\pi \boldsymbol{u})_\pi = \begin{bmatrix} \partial_1 u_1 - \kappa_1 u_2 - u_n K_{11} & \partial_1 u_2 + \kappa_1 u_1 - u_n K_{12} \\ \partial_2 u_1 + \kappa_2 u_2 - u_n K_{12} & \partial_2 u_2 - \kappa_2 u_1 - u_n K_{22} \end{bmatrix}. \tag{A 6}$$

The symmetric and skew-symmetric components are

$$S_{\alpha\beta} = \frac{1}{2}\begin{bmatrix} 2(\partial_1 u_1 - \kappa_1 u_2 - u_n K_{11}) & \partial_1 u_2 + \partial_2 u_1 + \kappa_\alpha u_\alpha - 2u_n K_{12} \\ \partial_1 u_2 + \partial_2 u_1 + \kappa_\alpha u_\alpha - 2u_n K_{12} & 2(\partial_2 u_2 - \kappa_2 u_1 - u_n K_{22}) \end{bmatrix}, \tag{A 7}$$

and

$$A_{\alpha\beta} = \frac{1}{2}\begin{bmatrix} 0 & \omega_n \\ -\omega_n & 0 \end{bmatrix}, \tag{A 8}$$

where, by (2.5),

$$\omega_n = \partial_1 u_2 - \partial_2 u_1 + u_1\kappa_1 - u_2\kappa_2. \tag{A 9}$$

Finally, we note that

$$r_s = \nabla_\pi\cdot\boldsymbol{u} = S_{11} + S_{22} = \partial_1 u_1 + \partial_2 u_2 - (\kappa_1 u_2 + \kappa_2 u_1) - u_n K, \tag{A 10}$$

where $K = K_{11} + K_{22}$ is twice the mean curvature.

REFERENCES

Aris, R. 1962 *Vectors, Tensors, and the Basic Equations of Fluid Mechanics*. Prentice-Hall.

Barthès-Biesel, D. & Sgaier, H. 1985 Role of membrane viscosity in the orientation and deformation of a spherical capsule suspended in shear flow. *J. Fluid Mech.* **160**, 119–135.

Batchelor, G. K. 1967 *An Introduction to Fluid Dynamics*. Cambridge University Press.

Caponi, E. A., Fornberg, B., Knight, D. D., Mclean, J. W., Saffman, P. G. & Yuen, H. C. 1982 Calculation of laminar viscous flow over a moving wavy surface. *J. Fluid Mech.* **124**, 347–362.

Caswell, B. 1967 Kinematics and stress on a surface of rest. *Arch. Ration. Mech. Anal.* **26**, 385–399.

Dishington, R. H. 1967 Rate of surface-strain tensor. *Am. J. Phys.* **33**, 827–831.

Edwards, D. A., Brenner, H. & Wasan, D. T. 1991 *Interfacial Transport Processes and Rheology*. Butterworth Heinemann.

Evans, E. A. & Skalak, R. 1980 *Mechanics and Thermodynamics of Biomembrances*. CRC Press, Boca Raton.

Pozrikidis, C. 1997 *Introduction to Theoretical and Computational Fluid Dynamics*. Oxford University Press.

Pozrikidis, C. 2001 Interfacial dynamics for Stokes flow. *J. Comp. Phys.* **169**, 250–301.

Scriven, L. E. 1960 Dynamics of a fluid interface. *Chem. Engng Sci.* **12**, 803–814.

Secomb, T. W. & Skalak, R. 1982 Surface flow of viscoelastic membranes. *Q. J. Mech. Appl. Maths* **35**, 233–247.

Slattery, J. C. 1990 *Interfacial Transport Phenomena.* Springer.

Waxman. A. M. 1984 Dynamics of a couple-stress fluid membrane. *Stud. Appl. Maths* **70**, 63–86.

Wu, J. Z. Tramel, R. W., Zhu, F. L. & Yin, X. Y. 2000 A vorticity dynamics theory of three-dimensional flow separation. *Phys. Fluids* **12**, 1932–1954.

Wu, J. Z. & Wu, J. M. 1996 Vorticity dynamics on boundaries. *Adv. Appl. Mech.* **32**, 119–275 (referred to herein as WW96).

Zhao, H., Wu, J. Z. & Luo, J. S. 2004 Turbulent drag reduction by travelling wave of flexible wall. *Fluid Dyn. Res.* **34**, 175–198.